Eur. Phys. J. D **10**, 423–431 (2000)

THE EUROPEAN PHYSICAL JOURNAL D

EDP Sciences

The pulse shape of a passively Q-switched microchip laser

T. Erneux[1,a], P. Peterson[2], and A. Gavrielides[2]

[1] Université Libre de Bruxelles, Optique Nonlinéaire Théorique, Campus Plaine, C.P. 231, 1050 Bruxelles, Belgium
[2] Air Force Research Laboratories, Nonlinear Optics Center of Technology, AFRL/DELO, 3550 Aberdeen Ave. SE, Kirtland AFB, NM 87117-5776, USA

Received 2 August 1999

Abstract. The shape of the intensity pulse of a passively Q-switched microchip laser is investigated numerically and analytically. Our analysis is motivated by independent microchip laser experiments exhibiting nearly symmetric pulses in the case of a semiconductor saturable absorber and asymmetric pulses in the case of a solid state saturable absorber. Asymptotic methods are used to determine limiting behaviors of the pulse shape for both symmetric and asymmetric pulses. In the first case, we determine a sech^2 solution parametrized by one parameter which can be determined by solving two coupled nonlinear algebraic equations. In the second case, the pulse solution is decomposed into two distinct approximations exhibiting different amplitude and time scales properties. We review earlier approximations of the repetition rate and the pulse width.

PACS. 42.65.Sf Dynamics of nonlinear optical systems; optical instabilities, optical chaos and complexity, and optical spatio-temporal dynamics – 42.55.Sa Microcavity and microdisk lasers – 42.60.Gd Q-switching

1 Introduction

In recent years there has been an increased interest in CW pumped passively Q-switched (PQS) microchip lasers because they are compact, simple to fabricate and they offer good lasing properties for scientific and industrial applications. In particular, PQS microchip lasers are now capable of producing extremely short high-peak-power pulses (*i.e.*, less than 1 ns duration and with peak powers larger than 10 kW). PQS microchip studies consider CW pumped devices which use either semiconductor [1–4] or solid state saturable absorbers [5–8]. In order to optimize the properties of these pulses, several parameters can be controlled such as the optical density of the absorber, the crystal thickness, or the pump power. Simple theoretical guidelines for the pulse width, the repetition rate and other measurable physical quantities are desirable but consist of either simple empirical formulae [2,6] or numerical simulations of laser rate equations [8]. The rate equations consist of three nonlinear first-order differential equations for the photon density, the laser population inversion, and the absorber state population. They cannot be solved exactly and their numerical integration can be delicate because of the PQS distinct time and amplitude scales. However, we may take advantage of these different scales and construct an asymptotic approximation of the PQS limit-cycle orbit in the phase plane [10]. In [12], we estimated the parameters for the experiment by Zayhowski and Dill III [6] and derived this approximation for microchip lasers. Specifically, we obtained a series of nonlinear algebraic equations for physically relevant quantities such as the pulse peak power and the repetition rate.

In this paper, we concentrate on the shape of the intensity pulse. The pulses observed in [6] are typically energetic and asymmetric. By contrast, the pulses observed by Spühler *et al.* [4] are less energetic and nearly symmetric. Both experiments are using microchip lasers but with different saturable absorbers. A first objective of this paper is to understand the similitudes and differences between these microchip laser experiments. To this end, we shall formulate the laser rate equations in dimensionless form and compute the parameters for the microchip lasers using either solid state saturable absorbers [6] or semiconductor saturable absorbers [4]. The values of these parameters suggest asymptotic limits which we investigate. Our analysis discusses the conditions for a nearly symmetric pulse and leads to a systematic derivation of its analytical approximation. We review and improve commonly used formulae for the amplitude and the width of the pulse. We also consider the case of a strongly asymmetric pulse and show that the pulse is the contribution of two distinct solutions. Each solution emphasizes a different physical process.

The plan of the paper is as follows. In Section 2, we formulate the laser rate equations in dimensionless form and discuss the values of the parameters which motivate a new analysis of the microchip laser equations. In Section 3,

[a] e-mail: terneux@ulb.ac.be

Table 1. Dimensionless parameters for microchip solid state lasers using two different absorbers.

saturable absorber	γ	$\overline{\gamma}$	$\overline{A}$	α	$A/A_{\rm th}$
Cr^{4+}:YAG	1.75×10^{-6}	6.35×10^{-5}	3.96	0.085 2	~ 2
semiconductor	3.7×10^{-7}	9.3×10^{-2}	0.36	4×10^{-3}	~ 2–3

we introduce the simplified equations for the PQS limit-cycle. These equations are obtained by a two part asymptotic analysis of the laser equations and form the starting point of our study of the pulse shape. We show that simple analytical expressions documented in the literature as guidelines for optimizing the pulse properties [2,4,8,11] can be derived from our reduced equations. In Section 4, we consider the case of symmetric pulses and derive a sech^2 pulse shape in a specific limit. The amplitude and the width of the pulse depends on one parameter which can be estimated either numerically or analytically. In Section 5, we investigate the case of an asymmetric pulse. We show that the intensity quickly increases and then slowly decays exponentially. Finally, we summarize the main points of our paper in Section 6.

2 Formulation

We consider the following dimensionless rate equations for a laser with a saturable absorber [13]

$$\frac{\mathrm{d}I}{\mathrm{d}s} = I\left(-1 + AD + \overline{AD}\right), \tag{1}$$

$$\frac{\mathrm{d}D}{\mathrm{d}s} = \gamma\big(1 - D(1+I)\big), \tag{2}$$

$$\frac{\mathrm{d}\overline{D}}{\mathrm{d}s} = \overline{\gamma}\left(-1 - \overline{D}(1+\alpha I)\right). \tag{3}$$

In these equations, I represents the intensity of the laser field, D is the dimensionless gain and $\overline{D}$ is the dimensionless saturable absorber gain. Time s is measured in units of the cavity round trip time $\tau_{\rm c}$. γ, $\overline{\gamma}$ are proportional to the decay rates of the two gains normalized by the cavity decay time. The parameter α is defined as the ratio of the gain saturation and saturable absorber saturation fluxes. $\overline{A}$ is the ratio of the saturable absorber small signal gain to the cavity losses. A is the dimensionless pump parameter associated with the active medium and is our control parameter. In terms of A, the laser first threshold is given by $A = A_{\rm th} \equiv 1 + \overline{A}$. These equations were used successfully for a series of studies concentrating on gas lasers with saturable absorber (see [14–16]). Modeling the microchip experiment of Zayhowski and Dill III [6] who are using a Nd:YAG gain medium coupled to a Cr^{4+}:YAG saturable absorber, we have estimated the values of the dimensionless parameters [12]. They are listed in the first line of Table 1. We also consider the microchip experiment of Spühler *et al.* [4] who used a diode-pumped Nd:YVO_4 microchip laser with a semiconductor saturable absorber. Values of the dimensionless parameters are evaluated in Appendix A and are listed in the second line of Table 1.

It is interesting to discuss the similitudes and differences between these two laser systems. Both lasers admit small values of γ, $\overline{\gamma}$, verify the inequality $\overline{\gamma} \gg \gamma$, and exhibit a small value of α. However, the value of $\overline{A}$ is different for these two lasers being relatively small in the case of a semiconductor saturable absorber. The small values of γ and $\overline{\gamma}$ are typical to all class B lasers which include CO_2, semiconductor and solid state lasers. The small value of α suggests a weak saturable absorber but, as we shall demonstrate, the fact that $\alpha\overline{\gamma}$ is $O(\gamma)$ or larger is sufficient to generate PQS oscillations. $\overline{A} \equiv q_0/l$ where $q = q_0$ is the equilibrium value of the saturable loss coefficient in the absence of laser light and l is the nonsaturable loss coefficient (see Appendix A). For the solid state saturable absorber, we determine the values of $q_0 = 2\sigma_a N_0 L_{\rm s}$ and $l = \ln(1/r)$ from the data collected in [12]. We note that q_0 is three times larger for the solid state saturable absorber ($q_{0\,\rm solid} \simeq 0.13$ and $q_{0\,\rm semi} \simeq 0.05$) while l is three time smaller for the solid state saturable absorber ($l_{\rm solid} \simeq 0.04$ and $l_{\rm semi} \simeq 0.14$). The two parameters q_0 and l both contribute to an $\overline{A}$ ten times larger for the solid state saturable absorber. The nonsaturable cavity losses clearly dominate in the case of a semiconductor saturable absorber while the saturable absorber is the main loss mechanism for a solid state saturable absorber.

With the parameter values listed in Table 1, we solve numerically equations (1–3) The long time solution corresponds to a limit-cycle shown in Figures 1 and 2. Its numerical integration is delicate when using conventional integration packages because the intensity is $O\big(\exp(-1/\gamma)\big)$ small during the interpulse phase. Therefore, we have determined the PQS oscillations by using a two part code. We integrate equations (1–3) by using a conventional method except when the intensity becomes small ($I < 10^{-3}$). Then, we use the exact solution of the linear equations obtained from equations (1–3) by setting $I = 0$ in equations (2, 3).

Integrating equations (1–3) for gradually smaller value of γ and $\overline{\gamma}$ ($\overline{\gamma}/\gamma$ fixed) clearly indicates an asymptotic limit for the PQS limit-cycle; see Figure 3. The figure shows that the maximum intensity scales like γ^{-1} while D remains $O(1)$ (*i.e.*, the limit cycle represented in terms of γI and D doesn't change as γ is decreased below 10^{-4}). The figure also shows that the intensity is almost zero during the interpulse period. With $I = 0$ into equation (2), we then note that D is a function of γt which implies that the interpulse period scales like γ^{-1}. The behavior of the limit-cycle for small γ thus suggests finding an approximation of the PQS oscillations in terms of two main contributions. These two contributions and their connection

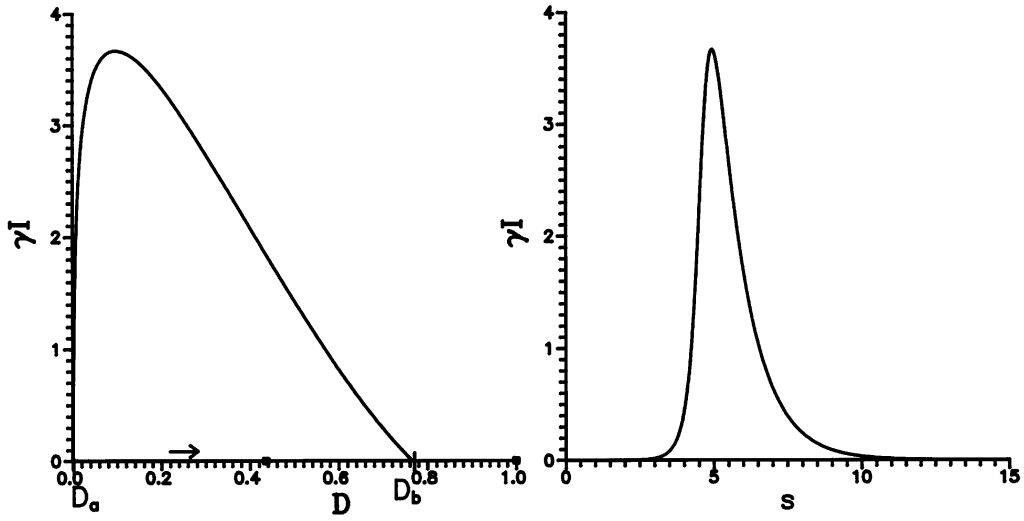

Fig. 1. PQS limit-cycle for a microchip laser using a solid state saturable absorber. The values of the parameters correspond to the first line in Table 1 and $A = 10.48$. Left: the limit-cycle is shown in the phase plane $(D, \gamma I)$. It consists of a long regime where $I \sim 0$ and D is slowly increasing (interpulse phase) followed by a quick change in the intensity (intensity pulse). The initial and final values of the interpulse regime occur at $D = D_a$ and $D = D_b$, respectively. The two squares denotes the singular points. Right: the asymmetric pulse shape.

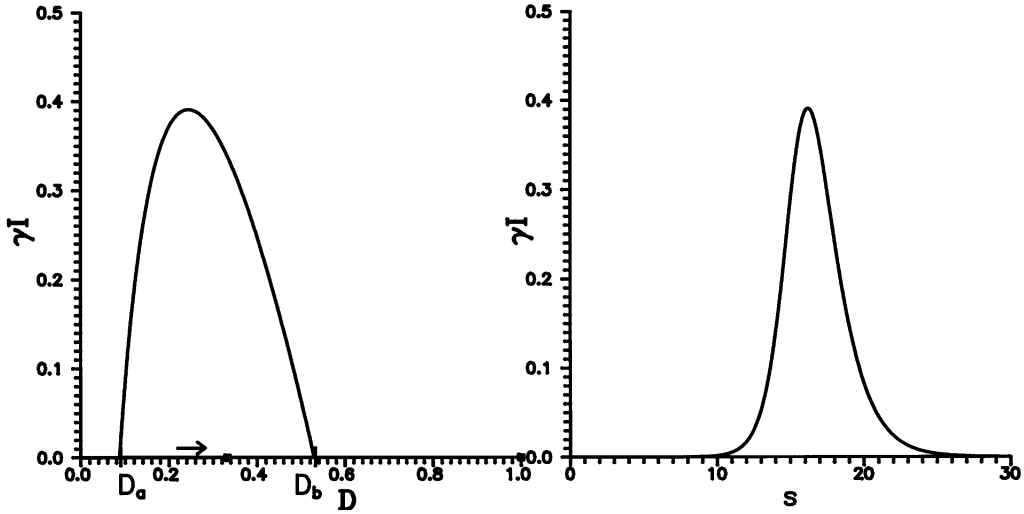

Fig. 2. PQS limit cycle for a microchip laser using a semiconductor saturable absorber. The values of the parameters correspond to the second line in Table 1 and $A = 4.08$. Left: the limit-cycle is shown in the phase plane $(D, \gamma I)$. Right: the nearly symmetric pulse shape.

(matching) can be determined by the method of matched asymptotic expansions [17].

3 Asymptotic approximation of the PQS limit-cycle oscillations

The asymptotic analysis of the PQS oscillations in the limit γ and $\overline{\gamma} = O(\gamma)$ small is described in detail in references [10,12] so that we only summarize the main results. PQS oscillations consist of a succession of high intensity pulses separated by long intervals where the intensity is almost zero. Taking advantage of these different scales, the PQS limit-cycle oscillations can be described by five nonlinear algebraic equations for the period and the initial and final values of D and $\overline{D}$ of the interpulse phase. However, we note from Table 1 that $\overline{\gamma} \gg \gamma$ for our two microchip laser systems which allows us to reduce our five equations to three equations which we now describe.

3.1 Interpulse period

We substitute $I = 0$ into equations (2, 3) and solve the resulting linear equations (1–3). The requirement that I remain small during the interpulse solution leads to three conditions relating the period T and the initial and final

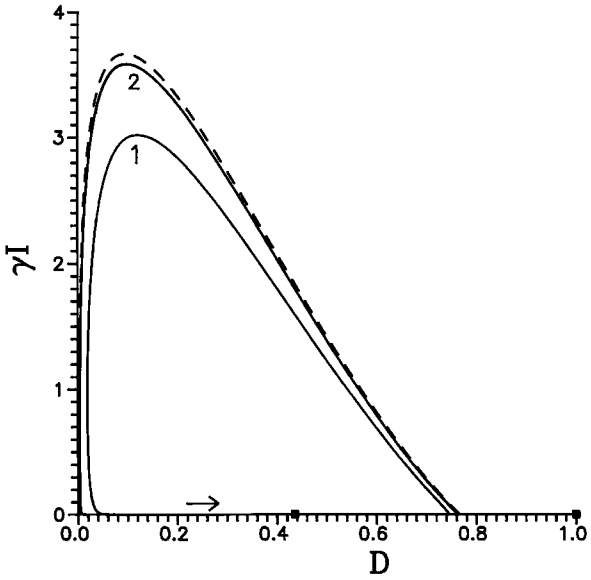

Fig. 3. Asymptotic limit of the PQS limit-cycle as $\gamma \to 0$. The limit-cycle solution has been determined for two different values of γ. The values of the parameters correspond to the first line of Table 1 except γ and $\overline{\gamma}$. Curve 1 corresponds to $\gamma = 1.75 \times 10^{-2}$, $\overline{\gamma} = 6.35 \times 10^{-1}$ and curve 2 corresponds to $\gamma = 1.75 \times 10^{-3}$, $\overline{\gamma} = 6.35 \times 10^{-2}$. For smaller γ, the numerical limit-cycle matches its asymptotic limit shown by the broken line and given by equation (10).

values of D and $\overline{D}$. Because $\overline{\gamma} \gg \gamma$, $\overline{D} \simeq -1$ as soon as $s = O(\gamma^{-1})$ and these three conditions reduce to two equations given by

$$(A - A_{\rm th})\gamma T + A(D_a - 1)\big(1 - \exp(-\gamma T)\big) = 0, \quad (4)$$

$$D_b = (D_a - 1)\exp(-\gamma T) + 1. \quad (5)$$

In these equations, $A_{\rm th} \equiv 1 + \overline{A}$ denotes the laser first threshold and $A > A_{\rm th}$. D_a and D_b denote the initial and final values of D, respectively (see Figs. 1 and 2).

We may eliminate T in equations (4, 5) and obtain an equation relating D_a and D_b only:

$$-(A - A_{\rm th})\ln\left(\frac{D_b - 1}{D_a - 1}\right) + A(D_a - D_b) = 0. \quad (6)$$

This equation will be useful when we analyze the behavior of D_a and D_b as functions of $\overline{A}$ (Appendix B).

3.2 High intensity pulse

The second contribution to the PQS oscillations comes from the high intensity pulse which now verifies the scaling $I = O(\gamma^{-1}) \gg 1$. Assuming $\overline{\gamma} = O(\gamma)$, the leading equations for the pulse are given by

$$I' = I\left(-1 + AD + \overline{AD}\right), \quad (7)$$

$$D' = -\gamma DI, \quad \overline{D}' = -\overline{\gamma}\alpha\overline{D}I \quad (8)$$

where prime means differentiation with respect to the inner time $\xi \equiv s - T$ $\big(\xi = O(1)\big)$. These equations are boundary layer (or inner layer) equations which must be solved with the matching conditions

$$I \to 0, \quad D \to D_b \quad \text{and} \quad \overline{D} \to -1 \quad (9)$$

as $\xi \to -\infty$. A first integration of these equations was obtained independently by Szabo and Stein [9], Erneux [10] and Degnan [11]. Specifically, we integrate the equations for $\mathrm{d}I/\mathrm{d}D$ and $\mathrm{d}\overline{D}/\mathrm{d}D$ and find: $\overline{D} = -(D/D_b)^m$ and

$$I = \frac{1}{\gamma}\left[A(D_b - D) + \ln\left(\frac{D}{D_b}\right) + \frac{\overline{A}}{m}\left(\left(\frac{D}{D_b}\right)^m - 1\right)\right] \quad (10)$$

where m is defined by

$$m \equiv \alpha\overline{\gamma}/\gamma. \quad (11)$$

A closed orbit in the phase plane implies that D and I match their starting values after a complete period. Equivalently, we require that $(D, I) = (D_a, 0)$ after the quick pulse. From (10), we then obtain an equation for $D = D_a$ given by

$$A(D_b - D_a) + \ln\left(\frac{D_a}{D_b}\right) + \frac{\overline{A}}{m}\left(\left(\frac{D_a}{D_b}\right)^m - 1\right) = 0. \quad (12)$$

We note from the values of the parameters listed in Table 1 that $m = 10^3$ for the semiconductor saturable absorber. This motivates a further simplification of equations (10, 12) given by

$$I = \frac{1}{\gamma}\left[A(D_b - D) + \ln\left(\frac{D}{D_b}\right)\right] \quad (m \text{ large}) \quad (13)$$

and

$$A(D_b - D_a) + \ln\left(\frac{D_a}{D_b}\right) = 0 \quad (m \text{ large}). \quad (14)$$

In summary, we derived three nonlinear algebraic equations for the interpulse period T and the initial and final points of the interpulse phase D_a and D_b. These equations are given by (4, 5, 12) or by (4, 5, 14) if m is large. They are appropriate for detailed analytical or numerical studies of the PQS oscillations. The solution of these equations represents the leading order approximation of the PQS limit-cycle and is based on the mathematical limit γ small and $\overline{\gamma} = O(\gamma)$ small. This limit is particularly appropriate for microchip lasers which exhibit very small γ. The analytical theories developed by Szabo and Stein [9] and later by Degnan [11] are not based on an asymptotic limit of the laser rate equations. They correctly found the leading equations for the high intensity pulse but fail to obtain an expression of the interpulse period that depends on the laser parameters only.

3.3 Near threshold conditions and gain reduction

In this subsection, we consider equations (4, 5, 14) for m large and show how simple expressions for the repetition rate and pulse width used in the literature can be derived. A good review of these expressions is given in [4]. Our analysis allows us to discuss their asymptotic validity and possible ways to improve them. Specifically, we investigate the limits of T, D_a and D_b near the laser threshold. Assuming $\gamma T \to \infty$ as $A - A_{\rm th} \to 0$ we find from (4, 5) that

$$\gamma T \simeq \frac{A(1-D_a)}{(A-A_{\rm th})} \tag{15}$$

and

$$D_b \simeq 1. \tag{16}$$

In the expressions (15, 16), the correction terms are $O\left(\exp(-(A-A_{\rm th})^{-1})\right)$ small. Then, from equation (14), we obtain D_a as the root of

$$A_{\rm th}(1-D_a) + \ln(D_a) = 0 \quad (m \text{ large}). \tag{17}$$

The expression (15) leads to the repetition rate $f_{\rm rep} = T^{-1}$

$$f_{\rm rep} = \gamma \frac{A - A_{\rm th}}{A_{\rm th}} \frac{1}{\Delta D} \tag{18}$$

where $\Delta D \equiv D_b - D_a \simeq 1 - D_a$ is defined as the gain reduction. The approximation (18) is equivalent to the expression of the repetition rate given by (12) in [4]. Similarly, (16) and (17) are equivalent to the expression (6) and equation (A11) in [4], respectively. It is instructive to further analyze equation (17) for D_a by considering the limit $\overline{A}$ small because it will allow us to find an expression of the gain reduction used in [4]. Specifically, expanding equation (17) for D_a close to 1, we find that

$$1 - D_a \simeq 2\overline{A}. \tag{19}$$

Since D_b is exponentially close to 1, we may write that the gain reduction $\Delta D = D_b - D_a$ equals $2\overline{A}$ which is equivalent to equation (7) in [4]. This particular limit (*i.e.*, first $A - A_{\rm th} \to 0$ and then $\overline{A} \to 0$) is however delicate because it requires the inequalities

$$0 < A - A_{\rm th} \ll \overline{A} \ll 1. \tag{20}$$

Practically, we would like to determine the behavior of the gain reduction as $\overline{A} \to 0$ for $A - A_{\rm th}$ arbitrary. In Figure 4, we show D_b and D_a obtained numerically from equations (6, 14). The gain reduction is clearly parabolic near $\overline{A} = 0$. In Appendix B, we determine this parabola analytically and find that

$$D_{b,a} \simeq \frac{1}{A}\left(1 \pm \sqrt{\frac{3\overline{A}(A-1)}{A}}\right) \tag{21}$$

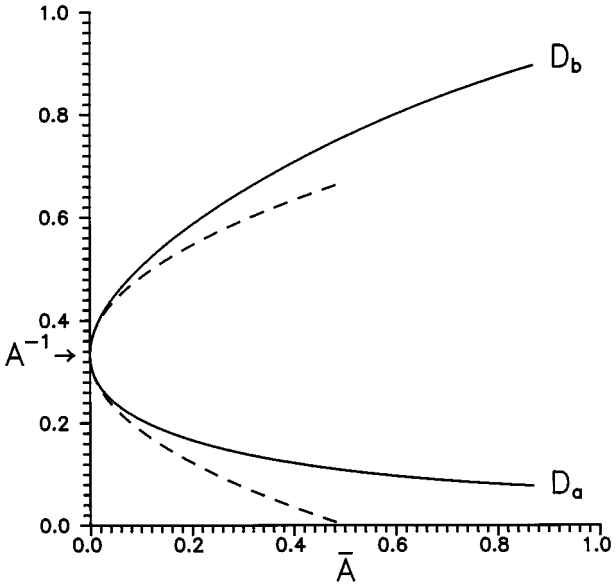

Fig. 4. The initial and final values of D of the interpulse regime as a function of $\overline{A}$. The points D_a and D_b are determined numerically from equations (6, 14). The dotted line is the small $\overline{A}$ limit given by (21).

as $\overline{A} \to 0$ (broken line in Fig. 4). In other words, the gain reduction $D_b - D_a$ scales like $\sqrt{\overline{A}}$ for the case

$$\overline{A} \ll 1 \quad \text{and} \quad A - A_{\rm th} = O(1) \tag{22}$$

and not like $\overline{A}$ as for the case (20).

The behavior of D_b and D_a becomes asymmetric as soon as $\overline{A} > 1$. This can be anticipated analytically from equations (6, 14) by determining D_b and D_a for $\overline{A}$ large. We find that $D_a \to 0$ and $D_b \to 1$ as $\overline{A}$ increases ($A = O(\overline{A})$) clearly implying asymmetry with respect to the line $D_b = D_a = A^{-1}$.

Although the expressions (10, 13) give the maximum intensity, it doesn't give the structure of the pulse as it varies in time. In order to find the pulse shape, a second integration is needed. An analytical expression of the integral solution in terms of elementary functions doesn't exist and we shall concentrate on particular cases.

4 Symmetric pulses

Spühler *et al.* [4] noted numerically that the intensity pulses are symmetric if $\overline{A} < 1$. An sech^2 fit of the pulse then allowed an estimation of the pulse width. In this section, we demonstrate analytically that a sech^2 intensity pulse is indeed the leading solution provided $\overline{A}$ is sufficiently small.

We consider the equation for D in (8) and substitute I given by (13). The resulting equation is

$$D' = -D\left[A(D_b - D) + \ln\left(\frac{D}{D_b}\right)\right]. \tag{23}$$

We solve this equation with the matching condition $D(-\infty) = D_b$ knowing that $D(\infty) = D_a$. The fact that $D_b - D_a \to 0$ as $\overline{A} \to 0$ (see (21)) motivates seeking a solution of the form

$$D = D_b(1 + \varepsilon u) \tag{24}$$

where ε is a small parameter defined by

$$\varepsilon \equiv AD_b - 1 \tag{25}$$

Substituting equations (24, 25) into equation (23), we find that the leading order problem for u as $\varepsilon \to 0$ is given by

$$u' = \frac{\varepsilon}{2}u(2 + u), \quad u(-\infty) = 0. \tag{26}$$

Solving equation (26), we obtain

$$u = -2\frac{\exp(\varepsilon\xi)}{1 + \exp(\varepsilon\xi)}\,. \tag{27}$$

Using equations (13, 23, 24), we have $I \simeq -\gamma^{-1}\varepsilon u'$ which then leads to

$$I = \gamma^{-1}\frac{\varepsilon^2}{2}\mathrm{sech}^2\left(\frac{\varepsilon\xi}{2}\right). \tag{28}$$

Note that this solution depends on one parameter only (ε). We may determine ε from the numerical determination of $D_b(\overline{A})$ (as in Fig. 4) or use its limit for $\overline{A}$ small given by

$$\varepsilon \simeq x_b \tag{29}$$

where x_b is defined by (B.10) in Appendix B. The expression (28) allows to formulate an expression for the pulse width given by

$$\Delta s = \frac{1}{\varepsilon}4\,\mathrm{arccosh}(\sqrt{2}) \simeq \frac{3.52}{\varepsilon}\,. \tag{30}$$

The expression (30) is equivalent to (8) in [4] provided $\varepsilon \simeq \overline{A}$ which is correct under the restrictive conditions (20).

In summary, we have shown analytically that a sech^2 intensity pulse is indeed the leading approximation of the laser equations provided that $\overline{A}$ is sufficiently small. The solution depends on one parameter (ε) which can be evaluated either numerically or analytically in the limit $\overline{A}$ small.

5 Asymmetric pulses

If $\overline{A}$ is progressively increased from a small value, the pulse shape quickly becomes asymmetric. In this section, we analyze this asymmetry by constructing an asymptotic solution for D. We substitute I given by (10) in the equation for D in (8) and find

$$D' = -D\left[A(D_b - D) + \ln\left(\frac{D}{D_b}\right) + \frac{\overline{A}}{m}\left(\left(\frac{D}{D_b}\right)^m - 1\right)\right], \quad D(-\infty) = D_b. \tag{31}$$

After solving equation (31), we determine the intensity using (10). In order to capture the asymmetry of the pulse, we propose to consider the limit A large (keeping $\overline{A}$ fixed). The solution is then the contribution of two distinct parts namely, a quick initial layer solution followed by a solution for its decay. We construct these solutions by using the method of matched asymptotic expansions [17]. The initial layer solution is obtained by seeking a solution of equation (31) of the form $X = D/D_b = X_0(\zeta) + A^{-1}X_1(\zeta) + \cdots$ where ζ is a fast time variable defined by $\zeta = AD_b\xi$. The leading order problem for X_0 is easily solved and gives

$$D = \frac{D_b}{1 + \exp(AD_b\xi)} + O(A^{-1}). \tag{32}$$

Substituting (32) into (10) and keeping the two first terms lead to the intensity

$$I_1(\xi) \simeq \gamma^{-1}\left[AD_b\frac{\exp\left(AD_b\xi\right)}{1 + \exp\left(AD_b\xi\right)} - \ln\big(1 + \exp\left(AD_b\xi\right)\big)\right] + O(1). \tag{33}$$

In the expression (33), D_b is a function of A which is determined from the interpulse period equations (see Appendix C). Note that $\overline{A}$ does not appear explicitly in (33) because (33) only shows the leading approximation of the intensity for A large. However, $\overline{A}$ appears implicitly through D_b. Note that as $AD_b\xi \to \infty$ (called the outer limit), D and I_1 approach the limits

$$D \to 0 \quad \text{and} \quad I_1 \to \gamma^{-1}\left[AD_b - AD_b\xi\right]. \tag{34}$$

These limits are needed in order to determine the solution after the quick initial layer. After the pulse reaches its maximum, it experiences a relatively slow decay. Substituting $D = \overline{D} = 0$ into equation (7), we now solve

$$I' = -I \tag{35}$$

with leads to the simple solution

$$I_2 = C\exp\left(-\xi\right). \tag{36}$$

In (36), C is a constant of integration which is determined by matching with the initial layer solution [17]. Specifically, we need to compare the behavior of (36) as $\xi \to 0$ (called the inner limit) with the outer limit (34). Expanding (36) for small ξ gives $I_2 = C(1 - \xi + \cdots)$. Comparing with (34) then leads to the condition $C = AD_b$ and

$$I_2 = \gamma^{-1}AD_b\exp\left(-\xi\right). \tag{37}$$

Figure 5 show the two functions (33, 37) together with an uniform solution. This uniform solution is best described

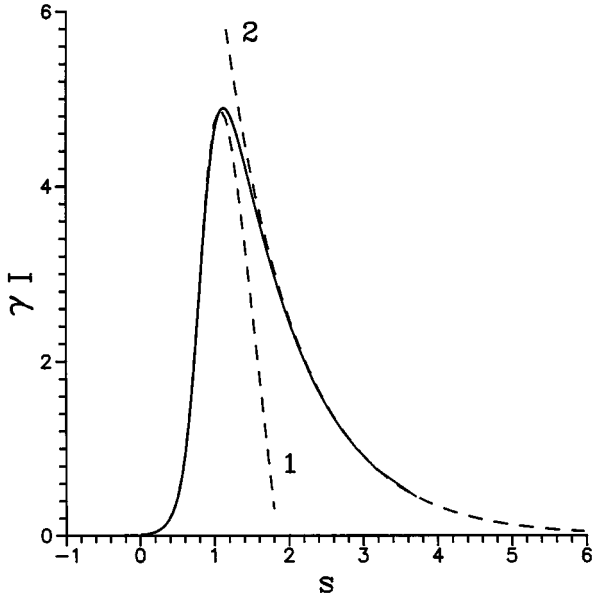

Fig. 5. Asymmetric intensity pulse. The figure represents the two approximations of the intensity pulse. They are labeled by 1 and 2 and are given by (33, 37), respectively. The full line represents the uniform solution (38, 39).

in parametric form and is given by[1]

$$\xi = \frac{1}{AD_b}\ln\left(\frac{D_b - D}{D_b}\right) - \ln\left(1 + \frac{1}{AD_b}\ln\left(\frac{D}{D_b}\right)\right) \quad (38)$$

and

$$\gamma I = A(D_b - D) + \ln(D/D_b) \quad (39)$$

where the parameter is D ($D_a < D < D_b$ where $D_a \ll 1$ is defined as the second root of the transcendental equation $A(D_b - D) + \ln(D/D_b) = 0$). We have found numerically that (37) is an excellent approximation of the decay of the pulse. On the other hand, (33) is in semi-quantitative agreement with the numerical solution for $A = 10.48$. The agreement becomes progressively better as we increases the pump A.

6 Summary

In this paper, we compared the dimensionless parameters of two distinct microchip laser experiments. We have noted similar orders of magnitudes for all parameters except for the saturable absorber pump parameter $\overline{A}$. In the case of a semiconductor saturable absorber, $\overline{A} < 1$ and symmetric pulses are observed numerically. In the case of a solid state saturable absorber, asymmetric pulses are observed with a much larger maximum.

In the first case, we confirm analytically that a sech^2 fit of the pulse is an asymptotic approximation of the laser rate equations. The sech^2 function depends on only one parameter which is a function of the laser pump parameters. It can be computed either numerically from two coupled nonlinear algebraic equations or analytically in the limit $\overline{A}$ small.

In the second case, we investigate the asymmetry of the pulse by considering the limit of large values of the laser pump parameter A. We find that the asymmetric pulse can be decomposed into two distinct functions. First, we note a quick initial increase of the intensity which is controlled by the pump parameter. Then, we note an exponential decay of the intensity which only depends on the decay rate of the field in the cavity. An exponential fit of the tail of the pulse could then lead to the cavity constant.

Our study of the PQS microchip laser oscillations differs from previous analytical investigations by the massive use of asymptotic methods. These methods allowed us to discuss the validity of previously used formulae and led to an unified description of the pulsating intensity oscillations in terms of various parameters.

The research of TE was supported by the US Air Force Office of Scientific Research grant AFOSR F49620-98-1-0400, the National Science Foundation grant DMS-9973203, the Fonds National de la Recherche Scientifique (Belgium) and the InterUniversity Attraction Pole of the Belgian government.

Appendix A: Dimensionless parameters for microchip lasers using semiconductor saturable absorbers

In this appendix, we consider the laser rate equations used by Spühler *et al.* [4] and reformulate these equations in the form of equations (1–3). The equations in [4] are formulated in terms of the laser power $P(t)$, the intensity gain coefficient per cavity round trip $g(t)$, and the intensity saturable loss coefficient per cavity round trip $q(t)$. They are given by

$$\begin{aligned} T_{\mathrm{R}}\frac{\mathrm{d}P}{\mathrm{d}t} &= [g - q - l]\,P, \\ \frac{\mathrm{d}g}{\mathrm{d}t} &= -\frac{g - g_0}{\tau_{\mathrm{L}}} - \frac{gP}{E_{\mathrm{L}}}, \\ \frac{\mathrm{d}q}{\mathrm{d}t} &= -\frac{q - q_0}{\tau_{\mathrm{A}}} - \frac{qP}{E_{\mathrm{A}}} \end{aligned} \quad (A.1)$$

where T_{R} is the cavity round-trip time, E_{L} is the saturation energy of the gain, τ_{L} is the upper-state lifetime of the gain medium, E_{A} is the saturation energy of the absorber, and τ_{A} is the relaxation time of the absorber. l denotes the total nonsaturable loss coefficient per round

[1] Using (32), we rewrite the first solution as $\xi = \xi_1(D) = (1/AD_b)\ln(D_b/D - 1)$. Then using equation (8) for D and (37), we have $\ln(D/D_b) = AD_b\big(\exp(-\xi) - 1\big)$ which gives $\xi = \xi_2(D) = -\ln\big(1 + (1/AD_b)\ln(D/D_b)\big)$. The common part (*i.e.*, $\lim \xi_1$ as $D \to 0 = \lim \xi_2$ as $D \to D_b$) is $\xi_{\mathrm{c}} = -(1/AD_b)\ln(D/D_b)$. Thus, the uniform solution is constructed as $\xi_{\mathrm{u}} = \xi_1 + \xi_2 - \xi_{\mathrm{c}}$ and is given by (38).

trip. $g = g_0$ and $q = q_0$ are the equilibrium values of g and q as $P = 0$. Typical values of the fixed parameters are [4]:

$$T_{\rm R} = 2.61 \text{ ps}, \quad l = 14\%, \quad \tau_{\rm L} = 50\ \mu\text{s}, \quad \tau_{\rm A} = 200 \text{ ps}, \quad \frac{E_{\rm L}}{E_{\rm A}} = 10^3, \quad q_0 = 5\%. \quad \text{(A.2)}$$

The pump parameter is defined by $r \equiv g_0 {g_{\rm c}}^{-1}$ where $g_{\rm c} \equiv l + q_0$ is the laser first threshold.

Introducing the new variables

$$D \equiv \frac{g}{g_0}, \quad \overline{D} \equiv -\frac{q}{q_0}, \quad I \equiv \frac{\tau_{\rm L}}{E_{\rm L}} P, \quad s \equiv \frac{l}{T_{\rm r}} t \qquad \text{(A.3)}$$

and the new parameters

$$A \equiv \frac{g_0}{l}, \quad \overline{A} \equiv \frac{q_0}{l}, \quad \gamma \equiv \frac{T_{\rm R}}{l\tau_{\rm L}}, \quad \overline{\gamma} \equiv \frac{T_{\rm R}}{l\tau_{\rm A}}, \quad \alpha \equiv \frac{\tau_{\rm A} E_{\rm L}}{\tau_L E_{\rm A}} \qquad \text{(A.4)}$$

into equation (A.1), we obtain

$$\frac{{\rm d}I}{{\rm d}s} = \left[AD + \overline{AD} - 1\right] I,$$
$$\frac{{\rm d}D}{{\rm d}s} = \gamma \left[1 - D - DI\right],$$
$$\frac{{\rm d}\overline{D}}{{\rm d}s} = \overline{\gamma} \left[-1 - \overline{D} - \alpha \overline{D} I\right]. \qquad \text{(A.5)}$$

We next evaluate the parameters (A.4) using (A.2) and $r = 3$. We find

$$\gamma = 3.7 \times 10^{-7}, \quad \overline{\gamma} = 9.3 \times 10^{-2}, \quad \overline{A} = 0.36, \quad A = r A_{\rm th} = 4.08, \quad \alpha = 4 \times 10^{-3} \qquad \text{(A.6)}$$

where $A = A_{\rm th} \equiv 1 + \overline{A}$ represents the laser first threshold.

Appendix B: The limit $\overline{A}$ small

In this appendix, we examine the limit $\overline{A} \to 0$ of our leading approximation for γ small. We assume $A - A_{\rm th} = O(1)$. As we shall demonstrate, we obtain two different limits if we consider the parameter $m = O(1)$ or if we consider m large.

B.1 Case m = O(1)

The equations that describe our approximation of the limit-cycle are two equations for D_a and D_b defined as the initial and final values of D for the interpulse phase. These equations are given by equations (6, 12). We solve these equations by introducing the new variables x_a and x_b defined by

$$D_a = \frac{1}{A}(1 + x_a) \quad \text{and} \quad D_b = \frac{1}{A}(1 + x_b). \qquad \text{(B.1)}$$

We substitute (B.1) into equations (12, 6), assume that x_a and x_b are $O(\overline{A})$ small, and obtain the following problems for x_a and x_b ($x_a \neq x_b$):

$$-\overline{A} + \frac{1}{2}(x_a + x_b) + \frac{(x_b - x_a)}{2}\big(x_b + \overline{A}(m-1)\big) - \frac{(x_b - x_a)^2}{3} + O\left(\overline{A}^3\right) = 0, \qquad \text{(B.2)}$$

$$\overline{A} - \frac{1}{2}(x_a + x_b) + \frac{(x_b - x_a)}{2(1-A)}(x_a - \overline{A}) + \frac{(x_b - x_a)^2}{3(1-A)} + O\left(\overline{A}^3\right) = 0. \qquad \text{(B.3)}$$

The leading order problem is $O(\overline{A})$ and is identical for the two equations:

$$-\overline{A} + \frac{1}{2}(x_a + x_b) = 0. \qquad \text{(B.4)}$$

To obtain a second condition for x_a and x_b, we add equations (B.2) and (B.3). The resulting equation is now $O(\overline{A}^2)$. After simplification, we have the condition

$$x_a - \overline{A} + x_b(1 - A) + (1 - A)\overline{A}(m-1) + \frac{2}{3}(x_b - x_a)A = 0. \qquad \text{(B.5)}$$

Finally, we solve equations (B.4, B.5) and obtain

$$x_b = \frac{\overline{A}}{A}\big(3m(A-1) + A\big) \quad \text{and} \quad x_a = 2\overline{A} - x_b. \qquad \text{(B.6)}$$

Note that the limit m large of (B.6) is singular because x_b becomes large in this limit. We need to reexamine this problem by taking the limit m large first and then the limit $\overline{A}$ small.

B.2 Case m large

The limit m large of our leading approximation of the limit-cycle orbit is given by equation (14). The other equations remain unchanged. As for the previous case, we wish to solve two equations for the unknown D_a and D_b which are given by equations (14, 6). After introducing (B.1) into these equations, we assume that x_a and x_b are $O(\sqrt{\overline{A}})$ small, and obtain the following problems for x_a and x_b

$$\frac{1}{2}(x_a + x_b) + \frac{(x_b - x_a)}{2}x_b - \frac{(x_b - x_a)^2}{3} + O\left(\overline{A}^{3/2}\right) = 0, \qquad \text{(B.7)}$$

$$\overline{A} - \frac{1}{2}(x_a + x_b) + \frac{(x_b - x_a)}{2(1-A)}x_a + \frac{(x_b - x_a)^2}{3(1-A)} + O\left(\overline{A}^{3/2}\right) = 0. \qquad \text{(B.8)}$$

From equation (B.7), we find that the leading order solution satisfies the condition

$$x_a + x_b = 0. \qquad \text{(B.9)}$$

In order to obtain a second condition, we add equations (B.7) and (B.8). Then solving for x_b using equation (B.9), we find

$$x_b = \sqrt{\frac{3\overline{A}(A-1)}{A}} \quad \text{and} \quad x_a = -x_b. \tag{B.10}$$

Appendix C: The limit A large

In the limit $A \to \infty$, D_a quickly approaches zero. From equation (6) with $D_a = 0$, we find that $D_b = D_b(A)$ satisfies the following equation

$$(A - A_{\rm th}) \ln(1 - D_b) + AD_b \simeq 0 \tag{C.1}$$

which we may analyze using the implicit solution $A = A(D_b)$

$$A = \frac{A_{\rm th} \ln(1 - D_b)}{\ln(1 - D_b) + D_b} \cdot \tag{C.2}$$

Finally, we obtain D_a from equation (12) as

$$D_a \simeq D_b \exp(-AD_b). \tag{C.3}$$

Equations (C.1, C.3) are valid provided $\exp(-AD_b) \ll 1$ which can be realized with moderate values of A. The extreme limit $A \to \infty$ gives

$$D_b \sim \frac{2A_{\rm th}}{(A - A_{\rm th})} \tag{C.4}$$

together with (C.3).

References

1. B. Braun, F.X. Kärtner, U. Keller, J.P. Meyn, G. Huber, Opt. Lett. **21**, 405 (1996).
2. B. Braun, F.X. Kärtner, G. Zhang, M. Moser, U. Keller, Opt. Lett. **22**, 381 (1997).
3. R. Fluck, B. Braun, E. Gini, H. Melchior, U. Keller, Opt. Lett. **22**, 991 (1997).
4. G.J. Spühler, R. Paschotta, R. Fluck, B. Braun, M. Moser, G. Zhang, E. Gini, U. Keller, J. Opt. Soc. Am. B **16**, 376 (1999).
5. J.J. Zayhowski, Opt. Lett. **21**, 588 (1996); Errata, Opt. Lett. **21**, 1618 (1996).
6. J.J. Zayhowski, C. Dill III, Opt. Lett. **19**, 1427 (1994).
7. J.J. Zayhowski, Opt. Lett. **22**, 169 (1997).
8. Y. Shimony, Z. Burshtein, A. Ben-Amar Baranga, Y. Kalisky, M. Strauss, IEEE J. Quant. Electron. **32**, 305 (1996).
9. A. Szabo, R.A. Stein, J. Appl. Phys. **36**, 1562 (1966).
10. T. Erneux, J. Opt. Soc. Am. B **5**, 1063 (1988).
11. J.J. Degnan, IEEE J. Quant. Electron. **31**, 1890 (1995).
12. P. Peterson, A. Gavrielides, M.P. Sharma, T. Erneux, IEEE J. Quant. Electron. **35**, 1 (1999).
13. A.E. Siegman, *Lasers* (Univ. Science Books, 1986), p. 1024.
14. E. Arimondo, F. Casagrande, L.A. Lugiato, P. Glorieux, Appl. Phys. B **30**, 57 (1983).
15. E. Arimondo, P. Bootz, P. Glorieux, E. Menchi, J. Opt. Soc. Am. B **2**, 193 (1985).
16. N. Abraham, P. Mandel, L. Narducci, Prog. Opt. **25**, 1 (1988); see p. 104.
17. C.M. Bender, S.A. Orzag, *Advanced Mathematical Methods for Scientists and Engineers* (McGraw-Hill Book, Comp. New York, 1978).